



# Martensitic transition and shape memory effect of Ti-Zr-Mo series alloys



S. Zhang, S.X. Liang\*, Y.X. Yin, L.Y. Zheng, H.L. Xie, Y. Shen

College of Materials Science and Engineering, Hebei University of Engineering, Handan 056038, China

## ARTICLE INFO

### Keywords:

TiZr-based alloy  
Martensitic transition  
Shape memory effect  
Phase transition  
Microstructure

## ABSTRACT

Development of shape memory alloys is always one of the most important directions for functional Ti alloys. The Ti-Zr-Mo series alloys with various Mo contents were prepared. The main aim of the current work is to investigate the effects of Mo on martensitic transition and shape memory effect of Ti-Zr alloy. The X-ray diffraction and transmission electron microscope results indicate that the phase constitution of the examined alloys is greatly dependent on Mo content. The Ti-Zr-Mo alloy with 2 wt% Mo is composed mainly of  $\alpha'$  martensite and a few  $\beta$  phase. As the Mo content increased to 4 wt%, the Ti-50Zr-4Mo alloy consists of  $\alpha''$  martensite and  $\beta$  phase. As the Mo content further increased to 8 wt%, the alloy consists mainly  $\beta$  phase and a barely detectable amount of  $\alpha''$  martensite. Thermal analysis shows that the reverse martensitic transition temperature of the examined alloys decreases with the increasing of Mo. The reverse martensitic transition start,  $A_s$ , temperature is approximately 584 °C for Ti-50Zr-2Mo alloy and 519 °C for Ti-50Zr-4Mo, respectively. And the martensitic transition start,  $M_s$ , temperature is approximately 553 °C and 501 °C for that two alloys, respectively. But no obvious exothermic and/or endothermic peak can be observed in DSC curve of Ti-50Zr-8Mo alloy. Furthermore, the effect of Mo content on shape memory recovery ratio,  $\eta$ , of the examined alloys was also investigated. Results show that the  $\eta$  first increases and then decreases with the increasing of Mo. The alloy with 4 wt% Mo has the maximum  $\eta$  approximately 13.8%. The influencing mechanism of Mo content on shape memory effect of the examined alloys was also discussed. This findings not only supplied a series of shape memory TiZr-based alloys, but also enriched and deepened the theory of shape memory effect.

## 1. Introduction

Shape memory alloy (SMA) is a kind of new metal functional material developed in recent decades. Its shape memory effect (SME) is receiving more and more attention and being widely researched. Apart from SME, favorable properties such as superelasticity, favorable damping capacity and other important properties of shape memory alloys enable it to be applied in electronic, chemical, medical devices, energetic, aerospace, etc. fields [1–4].

Titanium (Ti) alloys are one of the most important SMAs. The TiNi alloy as a representative of Ti-based SMAs has been widely investigating and applying thanks to its favorable integrated performance [5–7]. However, the release of Ni into organism will cause cytotoxicity, sensitization, and etc. severe physical harms and limit its development [8]. Until now, development of new Ti-based SMAs is still one of the most important directions of metal intelligent materials. The Ti-Nb based [9–11], Ti-Ta based [12], Ti-Mo based [13–15] and Ti-Zr based [16] SMAs are developed in recent years.

It is well know that TiZr binary alloys are completely solid solutions for both high-temperature  $\beta$  phase and low-temperature  $\alpha$  phase (or  $\alpha'$

martensite) [17]. But the shape memory strain of TiZr binary alloys is only 1.4% [16] which is relative low compared with other Ti-based SMAs. Generally, favorable SME of Ti alloys results from the martensitic transition between  $\beta$  phase (bcc) and  $\alpha''$  martensite phase (orthorhombic structure). In order to increase its SME, some  $\beta$  stabilizers were added into TiZr binary alloys to increase the  $\beta$  stability and obtain  $\alpha''$  martensite. Firstly, the typical  $\beta$  stabilizer of Nb was added. Cui et al. [18] showed that the maximum shape memory strain of Ti-20Zr-10Nb alloy is up to 2.5%. After that, elements of Fe and/or Ta were also added and the corresponding maximum shape memory strain is as large as 4.1% for Ti-19.5Zr-10Nb-0.5Fe alloy [19] and 3.3% for Ti-20Zr-10Nb-4Ta [20], respectively. Recently, the effect of addition of Mo, as a typical  $\beta$  stabilizer, on SME of TiZr binary alloys is being regarded highly gradually. Some findings about effect of Mo on SME of TiZr binary alloys were also reported [21–23]. However, there are still some unclear issues need to be investigated and lucubrated.

In this work, the microstructure and SEM of Ti-Zr-Mo alloys with various Mo were investigated and the influencing mechanism of Mo on martensitic transition and SME of Ti-Zr-Mo alloys are also discussed. This findings will have important promote effect on development of

\* Corresponding author.

E-mail address: [liangshx@hebeu.edu.cn](mailto:liangshx@hebeu.edu.cn) (S.X. Liang).

TiZr-based SMAs.

## 2. Materials and experimental procedure

Sponge Zr (Zr + Hf  $\geq$  99.5 wt%), high pure Ti (> 99.9 wt%), and Mo (> 99.9 wt%) were used to prepare the Ti-50Zr-*x*Mo (*x* = 2, 4, and 8, wt.%, abbreviated to M*x*) alloys. The raw materials were melted at least thrice by vacuum nonconsumable electro-arc furnace under argon atmosphere to ensure uniform chemical composition. The uniform ingots were remelted and suction casted into a water-cooled copper mold with a cavity dimension of  $\varnothing$  10 mm  $\times$  100 mm. The rod castings were sectioned into specimens with various shapes and sizes for next tests.

NETZSCH-STA449C/6/G type Differential Scanning Calorimetry (DSC) was used to determine the phase transition temperatures with heating and cooling rates of 10 °C/min in argon protection atmosphere. A small piece of specimen with weight of about 9 mg was cut from the center of rod casting and polished for DSC test. D/MAX-2500/PC type X-ray diffraction (XRD) using Cu K $\alpha$  radiation and JEM 2010 type Transmission electron microscope (TEM) were used to examine the crystal structure and phase constitution of various Ti-Zr-Mo alloys. OLYMPUS DSX500 type Opto-digitao Microscope (OM) was used for microstructural observation and analysis. The metallographic specimens were prepared according to the standard guide for preparation of metallographic specimens (ASTM: E3-11). SME of the examined alloys was determined on universal testing machines using bending method as showed in Fig. 1, and the detail description of bending test was consulted previous reports [24,25]. The shape memory recovery ratio  $\eta = \frac{\theta - \theta'}{\theta} \times 100\%$  was measured to express the SME. Various specimens with size of approximately  $\varnothing$  10 mm  $\times$  5 mm for XRD and OM,  $\varnothing$  10 mm  $\times$  50  $\mu$ m for TEM and 50 mm  $\times$  6 mm  $\times$  1 mm for bending test were sectioned from rod castings. All bending specimens were grinded successively using 240# to 1500# waterproof abrasive papers and polished using diamond paste. The bending deformation strain is unified as  $\varepsilon_b = h/d = 1/4 = 0.25$ , where *h* and *d* denotes the thickness and bending diameter, respectively. Deformation specimens was performed on a planar rolling mill. The rod castings were multi-pass rolled at room temperature with total rolling reduction of 50% without intermediate annealing. To avoid accidental results, at least three times tests for each measurement were performed on each alloy. The results showed in the script are the average or typical results.

## 3. Results and discussion

Fig. 2 shows XRD patterns of Ti-Zr-Mo alloys with various Mo contents. Based on relevant literature [26] and standard PDF cards #44-1288 and # 44-1294 of pure Ti, the diffraction peaks of common phases containing  $\alpha/\alpha'$ ,  $\alpha''$  and  $\beta$  phases in pure Ti are showed in Fig. 2(a). The XRD patterns of Ti-Zr-Mo alloys are showed in Fig. 2(b). XRD analysis shows that the M2 alloy is composed of prime  $\alpha'$  (or  $\alpha$ ) phase with close-packed hexagonal structure and a small amount of  $\beta$

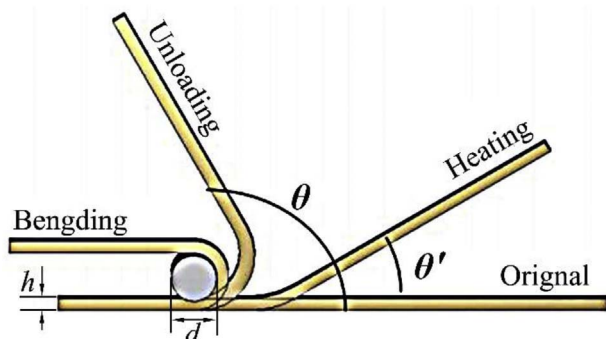


Fig. 1. The schematic diagram of bending measurement of shape memory recovery ratio.

phase with body-centered cubic structure. According to previous reports [16,27,28], water quenched TiZr binary alloys were composed mainly of  $\alpha'$  martensite. Although the M2 alloy contains  $\beta$ -stabilizer of Mo, its content of 2 wt% is insufficient to obtain  $\alpha''$  martensite. Kuroda et al. [23] also showed the similar results that the phase constitution of Ti-20Zr-Mo alloys is  $\alpha'$  phase without molybdenum,  $\alpha' + \alpha''$  (only 7%) phases with 2.5 wt% of molybdenum. As the Mo content increased to 4 wt%, the M4 alloy consists of  $\alpha''$  martensite with orthorhombic structure and retained  $\beta$  phase. As mentioned above, Mo is a typical  $\beta$  stabilizer for Ti and Zr alloys. Phase constitution of quenched Ti and/or Zr alloys will change as the order of  $\alpha' \rightarrow \alpha'' \rightarrow (\omega) \rightarrow \beta$  as Mo increased [23,29,30]. Thus, the martensite varies from  $\alpha'$  for M2 alloy to  $\alpha''$  for M4. As the Mo content further increased to 8 wt%, the  $\beta$  phase is wholly retained following the above mentioned order.

Micrographs of Ti-Zr-Mo alloys with various Mo contents are showed in Fig. 3. Results show that the microstructural feature of M2 alloy is acicular second phase separating out from the matrix phase. Based on the corresponding XRD result, the acicular phase is  $\alpha'$  martensite and the matrix is retained  $\beta$  phase. As the Mo content increased to 4 wt%, only some fine black dots can be observed in the matrix. Likewise, the fine black dots are  $\alpha''$  martensite according to the XRD result of M4 alloy. The similar result was also showed in previous reports [31–34]. As the Mo content further increased to 8 wt%, only  $\beta$  matrix can be observed in the OM micrograph.

To exhibit the microstructure more clear and accurate, the TEM was also used to determine the microstructure of Ti-Zr-Mo series alloys and results are showed in Fig. 4. The bright field image and corresponding electron diffraction proved that the precipitation is acicular  $\alpha'$  martensite in M2 alloy and fine lenticular  $\alpha''$  martensite in M4, respectively. That are the same with results of XRD and OM. However, a few of fine lenticular  $\alpha''$  grains were observed in the bright field image of M8 alloy in Fig. 4(c). That is, the M8 alloy contains rare  $\alpha''$  martensite which did not detected in XRD and OM. It is well know that XRD and OM have relatively low measuring precision. The amount of  $\alpha''$  martensite in M8 is too small to be detected and observed using XRD and OM. From the above, the phase constitution of Ti-Zr-Mo alloys changes as the order of  $\alpha' + \beta \rightarrow \alpha'' + \beta \rightarrow \beta + \alpha''$  (rare) as the Mo content increased from 2 wt% to 8 wt%.

The DSC results of Ti-Zr-Mo alloys with various Mo contents are showed in Fig. 5. Based on phase constitution and phase transition theory of Ti- and TiZr-based alloys, the endothermic peak in DSC curves indicates the reverse martensitic transition, namely, transition from martensite into  $\beta$  phase. Thus, the reverse martensitic transition start,  $A_s$ , and finish,  $A_f$ , temperatures of the examined alloys with various Mo contents can be obtained and results, as well as the  $A_s$  and  $A_f$  temperatures of Ti-45Zr alloy [16] for comparison, are showed in Table 1. The  $A_s$  and  $A_f$  temperatures of M2 is approximately 584 °C and 627 °C, respectively. The reverse martensitic transition temperatures of M2 alloy is low than Ti<sub>70</sub>Zr<sub>30</sub> [16] (equivalent to Ti-45Zr) and similar with Ti-20Zr-10Nb [18]. As the Mo content increased to 4 wt%, the  $A_s$  and  $A_f$  temperatures decreased to 519 °C and 580 °C, respectively. Al-Zain et al. [35] also showed the similar result that the reverse martensitic transition temperature of Ti-(21, 22)Nb alloys decreased rapidly with the addition of Mo. It is well known that Mo is a typical  $\beta$  stabilizer for Ti- and TiZr-based alloys. Consequently, the phase transition temperature will decrease with the increasing of Mo. Besides, the endothermic peak intensity in DSC curve of M4 alloy is obviously weak than that of M2. Based on DSC testing theory, the intensity of endothermic peak in DSC curves is related to the phase transition enthalpy and mass of testing sample. All DSC specimens in this work have similar weight (~9 mg). Thus, the effect of mass of sample on intensity of endothermic peak can be neglected. The phase transition enthalpy is close related to transition process and amount of transition. The phase transition in M2 alloy is from  $\alpha'$  martensite into  $\beta$  phase during heating, but is from  $\alpha''$  into  $\beta$  in M4. Thus, the phase transition process between M2 and M4 alloys is completely different. Otherwise,

Download English Version:

<https://daneshyari.com/en/article/5457505>

Download Persian Version:

<https://daneshyari.com/article/5457505>

[Daneshyari.com](https://daneshyari.com)